Proceedings of the 4th WSEAS International Conference on Fluid Mechanics and Aerodynamics, Elounda, Greece, August 21-23, 2006 (pp349-354)

Numerical Simulation of Transient flow through Single Blade Centrifugal Pump Impellers with Tipgap Leakage

BRIAN DE SOUZA, JOHN DALY, ANDREW NIVEN and PATRICK FRAWLEY
John Holland Research Centre
Department of Mechanical and Aeronautical Engineering
University of Limerick
IRELAND

Abstract: - This paper is concerned with the application of Computational Fluid Dynamics (CFD) to a low specific speed (N_s=60) single blade impeller. Single blade centrifugal pump impellers are the extreme example of impeller design, with gross deviation from conventional design practice. A time accurate three-dimensional viscous flow simulation is performed, using the multiple frames of reference sliding mesh technique, at different flow rates (q= Q/Q_{design}= 0.5 to 1.5) and varying tip gap clearances. Time marching is controlled through the use of an implicit Second Order Backward Euler scheme with a physical timestep, corresponding to 6° impeller rotation. A hybrid prism / tetrahedral mesh is used in order to provide adequate grid resolution in the turbulent boundary layer while scalable wall functions are used to model the near wall region. The results obtained show quantitative agreement with physical test results in terms of global performance characteristics such as head developed and power consumption. One particular phenomenon highlighted in the results is the periodic pressure fluctuation due to interaction between impeller and volute. This is significantly exaggerated by the single blade impeller. The steady state, symmetric flow assumptions upon which Euler's pump and turbine equation are based are clearly violated for single blade impellers.

Key-Words: - CFD, Transient, Unsteady, Hydraulic, Wastewater, Pump, Turbomachinery

1 Introduction

Throughout the history of turbomachinery, fans, compressors, turbines and pump impellers have become characterized by large numbers of blades. Indeed, the most fundamental equation of all used in turbomachinery design, Euler's Equation, is based on the principle of having an infinite number of impeller blades such that the flow through the impeller can be regarded as radial, symmetric and of steady state. In reality, a finite number of blades are used. This distorts the flow pattern through the impeller, causes a relative eddy between the suction and pressure surfaces of the blades, and for pumps leads to a diminished actual pump head relative to the theoretically predicted Euler value. This phenomenon is taken into account in prominent conventional impeller design methods such as those presented by Stepanoff [1] or Troskolanski et al. [2] through the use of slip factors. Busemann [3], Pfleiderer [4], Stodola [5] amongst others have provided, through theoretical analysis, derivations from which slip factors can be calculated dependent on the number of blades used. The inaccuracy of slip factors, and the conventional design approach in general, increases with reducing blade numbers. Single blade impellers are thus the extreme example of impeller design.

The development of single blade impellers has come about as a response by pump manufacturers to the needs of the wastewater industry. One of the key requirements when pumping wastewater containing liquid / solid mixtures is that a required solids passage area is provided (Fig.1). The use of a single blade impeller, in combination with radical departures from conventional empirical geometrical design ratios, for example a greatly increased outlet height to inlet diameter ratio, allows for this solids passage area.

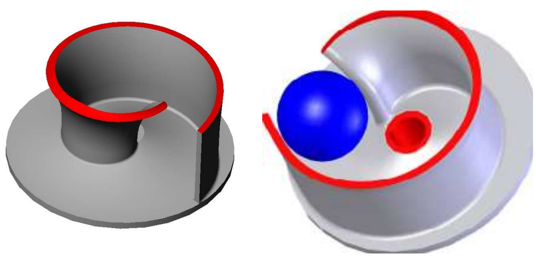

Fig 1: Prototype Impeller under investigation and Solids Passage Requirement

In this paper, the numerical simulation methodology is presented as applied to a prototype semi open, low specific speed (N_s=60) single blade impeller.

2 Previous Work

The application of computational fluid dynamics to turbomachinery has become increasingly common in recent years as manufacturers seek to optimize their product performance. Experimental centrifugal pump impeller investigations are complicated by the unsteady nature of the flowfield, the high-speed rotation of the impeller within the volute which makes pressure tapping of the impeller difficult, as well as the complicated three dimensional shape of the impeller. The reduction in CAD to mesh to solution cycle time in recent years has allowed CFD to participate in design [6] and become an essential tool for the hydrodynamic analysis of pumps.

There is very little published data, if any, available as regards the application of CFD to single blade impellers. A review of published literature however, shows a volume of studies concerning related conventional multi blade designs. Of these, two main groupings of CFD simulations can be determined, those being quasi-steady and full transient simulations. Quasi-steady CFD simulations assume the relative position between the impeller and volute is fixed in time and space, and any circumferential variation due to change in the relative position of the components is ignored. This approach has the advantage of being less computationally intensive than full transient solutions; however, it can induce inaccuracy in the final solution. Examples of quasi-steady simulations include the work of Liu et al. [7] who modeled a compressor with low solidity vanes at different operating conditions and Schachenmann et al. [8] who carried out a quasi steady study of three commercially available navier stokes codes with comparison to Laser Doppler Anemometry (LDA) measurements for a low specific speed radial pump impeller with vaned diffuser. More recently, quasi-steady studies have been carried out by Issa et al. [9] and Shukla et al. [10]. These have examined the effect of grids, numerical schemes and turbulence models on a low-pressure centrifugal fan and an end suction centrifugal six-vane pump respectively. Again, these included comparison with experimental data.

The operation of a conventional centrifugal pump is inherently an unsteady process. Quasi-steady simulations often show reasonable qualitative but poor quantitative agreement with experimental test data. This is especially true where the flowfield demonstrates considerable transient behavior. Unsteadiness in the flow is exaggerated by operating off design operating point, by having varied blade periodicity, where there are low blade numbers in the impeller or where there is considerable interaction between the impeller and volute regions, especially at the cutwater.

Several fully transient numerical simulations have been undertaken which capture and quantify the unsteady interaction and predict the pressure fluctuations for conventional centrifugal pumps. Some of the studies consider the flow to be inviscid, for example Hillewaert and Van der Breambussche [11]. This reduces the complexity of the flow enormously, however, the results obtained from this study, once again, were found to be only qualitatively acceptable when compared to experimental data. More recent studies have taken advantage of improved computational algorithms as well as hardware development in order to provide complex transient three dimensional turbulent flow simulations throughout the entire pump, with excellent quantitative agreement to experimental test results. Examples include Zhang et al. [12], Gonzalez et al. [13], Cui [14], Peters and Sleiman [15] and Koumoutsos et al. [16].

The effect of tipgap is detrimental to semi open impeller performance but is normally impossible to completely eliminate in experimental test. Several studies have experimentally investigated its effect, including Tamm and Stoffel [17], who looked at the influence of gap clearance on the leakage loss in a low speed centrifugal pump and Engin and Gur [18] who looked at the performance characteristics of shrouded and unshrouded centrifugal pumps with running tip gap clearances pumping liquid / solid mixtures. While tip gap leakage has been numerically studied in terms of axial flow pumps [19], it is a computationally expensive challenge due to the scale of the flow being resolved. For this reason, sparse literature is available as regards the modeling of CFD tip clearance flow in centrifugal pumps.

3 Numerical Methodology

The impeller under consideration in this study is a prototype low specific speed single blade design and is shown in Fig. 1. Three different tipgap configurations are presented corresponding to no tip gap, 1% and 2% blade height. Analysis of transient rotating flow with tipgap clearance is computationally expensive. In order to achieve a tolerable computational time, an 18-processor cluster was used. The methodology presented here is in accordance with the best practice guidelines as given in [20].

3.1 Computational Grid Generation

Three-dimensional CAD representations of the entire pump geometry were developed for each tip gap clearance configuration. The commercially available Ansys ICEM CFD 5.1 package was used for grid generation of the computational models. A direct CAD interface allowed for accurate importation of surface and curve geometry [6] without the need to resort to geometry cleanup operations. The overall flow domain throughout the pump was divided into three separate regions in order to make use of the multiple frames of reference technique. These regions included the inlet, which was extended over one-pipe diameter upstream of the impeller inlet to allow for developed flow, the impeller region, which was modeled separately for each tip gap clearance configuration, and the volute region. The outlet was extended downstream three pipe diameters to allow for uniform flow.

The meshing strategy adopted was to use a hybrid-meshing scheme consisting of prism and tetrahedral cells in the inlet and volute regions. Prism cells were extruded from wall surfaces, providing detailed resolution of the boundary layer as well as excellent geometrical definition of key features such as the impeller leading edge, while tetrahedral cells provided the core volume mesh. Fig. 2 shows this meshing strategy as applied to the impeller domain. This approach has the advantage over structured grids in that it can easily conform to difficult geometries. Also numerical diffusion errors for tetrahedral grids are consistent and are of the same order throughout the entire domain. This is not the case for structured grids, which can thus cause false confidence. While tetrahedral grids generally do incur higher numerical diffusion than hexahedral grids with similar cell numbers, this discrepancy diminishes rapidly with second order numerical discretisation.

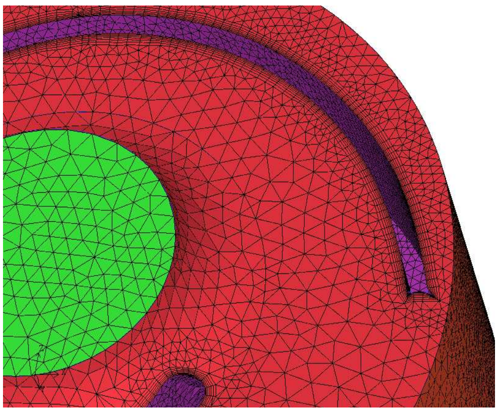

Fig 2: Hybrid Meshing scheme with layers of prism elements extruded from the blade surface.

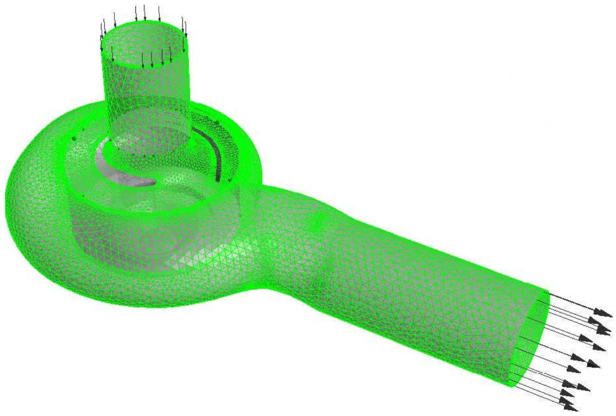

Fig 3: Entire Computational Domain, consisting of inlet, impeller and volute regions

In total, 24K tetra / 16k prism cells were used in the inlet domain and 407k tetra / 105k prism cells were used in the volute domain. In the impeller region, a hybrid mesh consisting of 436K tetra / 209K prism cells was used for the no tip gap clearance configuration. Extrusion of prism cells from the blade surface was not possible with the 1% and 2% tip gap configurations as this extended beyond the volume of the domain. Instead, the global tetrahedral mesh size was reduced, requiring 3065k and 1042k cells respectively. This provided adequate resolution of the boundary layer and tipgap regions. Grid refinement studies applied to the no tipgap configuration demonstrated the insensitivity of the recorded global performance parameters with grid size for large grids. This grid insensitivity was strongly assisted by the use of scalable wall functions.

3.2 Solver and Boundary Conditions

The commercially available CFX 5.7.1 code was employed for this study. The flow solver of the code applied, for turbulent incompressible flow, the continuity equation and the three-dimensional time-averaged Navier Stokes equations. In this study, the eddy viscosity assumption was used to model the Reynolds stresses. The eddy viscosity was determined by means of the standard k-ε turbulence model. The walls were modeled using a log-law scalable wall function approach as described by Esch and Menter [21]. This approach removed the lower limit on the near wall grid resolution imposed by standard wall functions. In combination with automatic wall treatment, Menter [22], this ensured that the grid could never be over refined in the boundary layer. An automatic switch between the low Reynolds formulation and wall functions was carried out based on the grid resolution provided to the code. The transport equations were discretised using a second order element based conserved finite volume method.

The numerical calculations were carried out with a multiple frames of reference approach whereby the impeller flow field was solved in a rotating frame, the inlet and volute in a fixed one. The two frames of reference were connected through the use of GGI fluid-to-fluid grid interfaces using the transient rotor stator formulation in accordance with best practice guidelines [20]. These connections were first order accurate, and their position updated at every timestep. The transient rotor stator approach ultimately accounted for all the interaction between the two frames.

The following boundary conditions were used. At the inlet of the computational domain the mass flow rate normal to boundary was set based on the design flowrate of the impeller, and adjusted in later simulations to capture the entire head/flow curve. The turbulence intensity at inlet was assumed to be in the order of 5%, which is typical for such turbomachinery [20]. At the outlet, an outflow boundary condition was used with a fixed static gage pressure reference value of 0 Pa averaged across the entire boundary. Both in fixed frame and in rotating frame the solid walls, i.e the impeller blades, hub, shroud, volute walls, and walls of the suction inlet were modeled using a no slip boundary condition. Monitors were set up to record average total pressures across inlet and outlet.

The time step of the unsteady calculations was set to 6.591×10^{-4} seconds. The time step is related to the rotational speed of the impeller and was chosen in such a way that one complete revolution of the impeller required approximately 60 timesteps. The chosen time step was small enough to get detailed time resolution, while minimizing computational expense. The number of iterations in each time step was set to four. This number of iterations was in most cases sufficient to reduce the maximum residuals by about three orders of magnitude. The average values of residuals (RMS values) were reduced by approximately four orders of magnitude. The second order backward Euler implicit transient time stepping scheme was selected which is bounded, conservative in time and implemented as:

$$\frac{\partial}{\partial t}\left(\int_{v} \rho\phi dv\right) = \frac{\rho V}{\Delta t}\left(\frac{3}{2}\Phi - 2\Phi^{0} + \frac{1}{2}\Phi^{00}\right) \qquad (1)$$

Calculations were carried out for almost ten impellers revolutions i.e for 600 timesteps at which point the solution was seen to be periodically stable. The head generated across the pump calculated through averaging of the differential pressure between inlet and outlet across the two final impeller revolutions:

$$H = \frac{\Delta P}{\rho g} \qquad (2)$$

The hydraulic efficiency was similarly averaged:

$$\eta = \frac{\rho g H Q}{\tau\omega} \qquad (3)$$

4 Experimental Pump Test

Physical experimental testing was carried out on the prototype impeller using a commercial wet test facility with a capacity of $250m^3$ in accordance with ISO 9906 Annex A1 [23]. The measurement of discharge pressure was recorded by means of calibrated industrial pressure transducers, while the flowrates were determined through the use of a magneto-inductive flow meter. Stable average measurements were obtained through heavy sampling and numerical averaging of the output signals over a number of revolutions. Bottomplate adjustment was carried out to minimize the tipgap clearance between the impeller and bottomplate.

5 Results and Discussion

To analyze the overall performance of the numerical method, the predicted non-dimensional global time averaged parameters of head, power consumption and efficiency are presented incorporating various tipgap clearances with comparison to experimental data. In Fig.4, below, the non-dimensional head / flow curves are presented. In all tipgap configurations the numerical simulations predict the correct trend of the curve, however the results are offset from the experimental values in accordance with tipgap. The ideal zero tipgap model over predicts the pressure generated by the pump across the curve. The 1% blade height tipgap model shows excellent agreement with experimental data, while the 2% blade height tipgap model over compensates for tipgap resulting in an under prediction of head developed across the operating range of the pump.

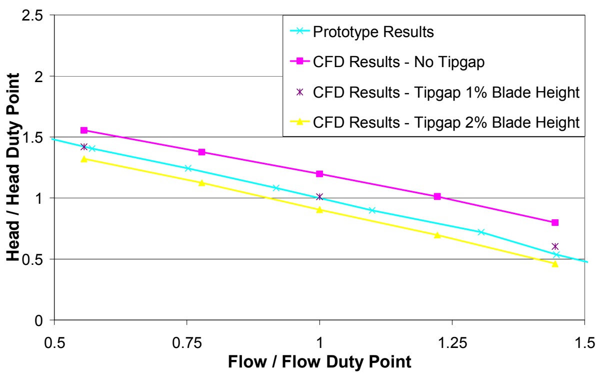

Fig 4: Non-dimensional Head / Flow Curves.

The numerically predicted power consumption is fundamentally dependant on accurate representation of the near wall region and especially the viscous shear stress distribution on the blade. The excellent agreement between numerically simulated and experimental results seen in Fig.5 justified the efforts in resolving the boundary layer. The non-dimensional power flow curve is influenced by tipgap clearance to a greater extent at higher flow rates, where the pump head is low. The 1% blade height tipgap model again provides the best agreement with experimental data.

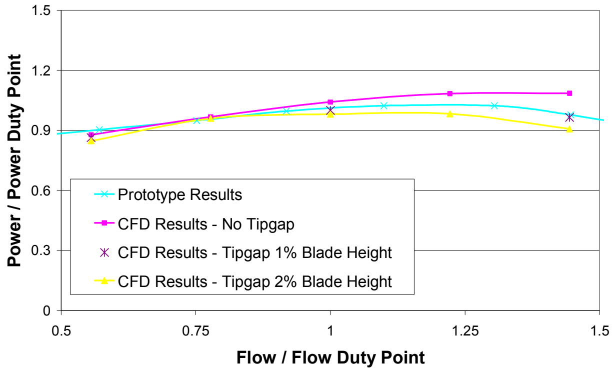

Fig 5: Non-dimensional Power / Flow Curves.

The final global parameter presented here is the non-dimensionalised efficiency versus flowrate.

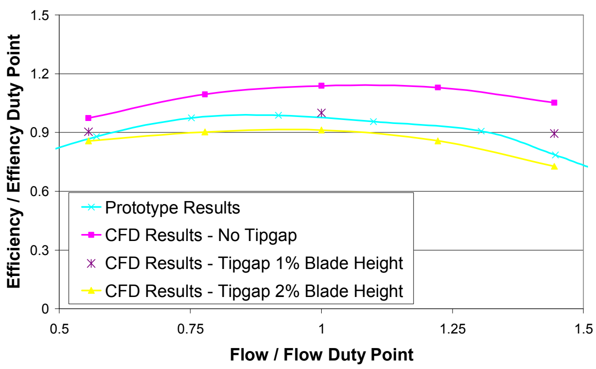

Fig 6: Non-dimensional Efficiency / Flow Curves.

What can clearly be seen in Fig. 6 is the detrimental impact of the tipgap clearance on hydraulic efficiency. While it is impossible to eliminate tipgap completely due to manufacturing considerations, the zero tipgap numerical simulation results illustrate the potential efficiency improvement that this could bring about.

5.1 Time Dependant Variations

Figs.4, 5 and 6 presented values of non-dimensional head, power and efficiency which were developed through averaging of the numerical simulation results at each tipgap configuration and flow rate, across the two final impeller blade rotations. Examination of the convergence plots for head developed across the pump shows clearly that the single blade impeller provides a strongly transient flow. The numerical solution converges towards a periodically stable pressure wave, as can be seen in Fig. 8.

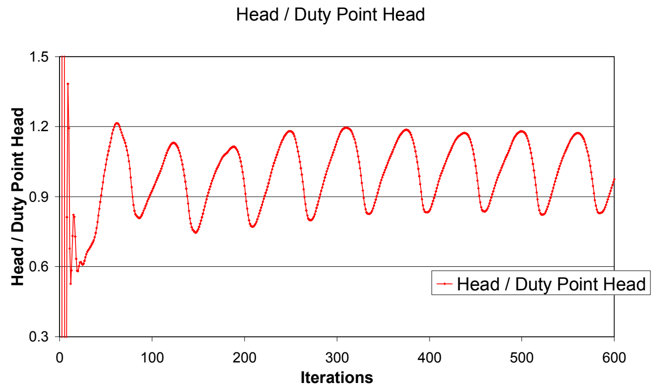

Fig 8: Convergence History of Pump Head (Tipgap 1% blade Height, Q_{design})

The magnitude of the pressure fluctuation ($0.3H/H_d$), which is seen, is much greater than that which is recorded with conventional impeller pumps. Pressure within the pump appears to build as the impeller trailing edge passes the cutwater of the volute, rising to a maximum value as the trailing edge approaches a ninety-degree angle to the cutwater, and then begins to decrease back towards its initial value and position.

A high-speed pressure pulsation dry test rig has recently been developed to capture the periodic pressure pulsations generated by the single vane impeller. This incorporated a high speed data acquisition unit in combination with a shaft mounted 13 bit encoder, high speed pressure transducers and a custom manufactured venturi measuring device. Experimental analysis of the phenomena is ongoing.

6 Nomenclature

g	= Gravity
H	= Overall head developed by pump
N	= Rotational rate
N_s	= Specific Speed ($NQ^{1/2}/H^{3/4}$)
ΔP	= Pressure rise across Pump
Q	= Flowrate
t	= Time
V	= Volume
Φ	= General Scalar Variable
ρ	= Density
τ	= Torque
ω	= Angular speed
°	= Current Solution time
°°	= Previous time

7 Conclusion

This research expands on the current state of the art in terms of single blade impeller design. It provides an example of how it is now possible, through the use of computational fluid dynamics to solve unsteady highly three-dimensional viscous flow in the entire impeller and volute casing of a centrifugal pump at and off design point. The results illustrate the effect of tipgap clearance, with increasing tipgap clearances proving detrimental to hydraulic performance. It highlights the significance of periodically unsteady flow phenomena to the single blade impeller.

References:

[1]Stepanoff, A.J, *Centrifugal and Axial Flow Pumps: Theory, design and Application*, 2nd Ed., Chapman and Hall, 1957.

[2]Lazarkiewicz, S., Troskolanski, A. T, *Impeller Pumps: Selection, Systems and Application*, Pergamon Press, 1965

[3]Busemann, A., *Das Förderhöhenverhältniss Radialer Kreiselpumpen Mit Logarithisch-spiraligen Schauflen*, Z. Angew Math. Mech, 1928, pp.371-381.

[4]Pfleiderer, C., *Die Kreiselpumpen fur Flussigkeiten und Gase*, 1st Ed., Springer, Berlin, 1924, pp.937

[5]Stodola, A., *Steam and Gas Turbines*, McGraw-Hill, 1927.

[6]Dawes, W.N, Dhanasekaran, P.C, Demargne, A. A, Kellar, W.P and Savill, A.M, *Reducing Bottlenecks in the CAD-to-Mesh-to-Solution Cycle Time to Allow CFD to Participate in Design*, Journal of Turbomachinery, Vol.123, July 2001, pp552-557

[7]Liu, Z., Hill, D.L., and Biba, Y., *Problem Diagnostics and Aerodynamic Improvement of a Field Compressor*, International Mechanical Engineering Congress & Exposition of ASME, Orlando, 2000.

[8]Schachenmann, A and Muggli, F., *Comparison of three Navier stokes codes with LAD measurements on an industrial Radial Pump Impeller*, FED-Vol 154, Pumping Machinery, ASME, 1993

[9]Issa, R.I and Xi, G., *Simulation of the Three dimensional Turbulent flow inside a Centrifugal Fan Impeller*, FED-Vol 238, Fluids Engineering Division Conference, ASME, 1996.

[10]Shukla, S.N and Kshirsagar, J.T, *Numerical Experiments of a Centrifugal Pump*, Proceedings of ASME FED SM, Quebec, Canada, 2002

[11]Hillewaert, K., Van der Braembussche, R.A., *Numerical Simulation of Impeller-Volute Interaction in Centrifugal Compressors*, Journal of Turbomachinery, Vol. 121, 1999, pp 603-608

[12]Majidi, M., *Numerical Study of Unsteady Flow in a Centrifugal Pump*, Journal of Turbomachinery, Vol.127, April 2005, pp363-371.

[13]Gonzalez, J., Fernandez, J., Blanco, E., Santolaria, C., *Numerical Simulation of the Dynamic Effects due to Impeller Volute Interaction in a Centrifugal Pump*, Journal of Fluids Engineering, Vol.124, June 2002, pp348-355.

[14]Cui, M., *Comparative Study of Unsteady Flows in a Transonic Centrifugal Compressor with Vaneless and Vaned Diffusers*, GT-0297, ASME, 2001.

[15]Peters, M., Sleiman, M.A., *Numerical Investigation of the Unsteady flow in Centrifugal Stages, GT-426*, ASME, 2000.

[16]Koumoutsis, A., Tourlidakis, A., Elder, R.I, *Analysis of unsteady Flow Interactions in a Centrifugal Compressor Stage*, GT-460, ASME 2002.

[17]Tamm, A., Stoffel, B., *The influences of Gap Clearance and Surface Roughness on Leakage loss and Disc Friction of Centrifugal Pumps*, Fluids Engineering Division Conference, ASME, 2002.

[18]Engin, T., Gur, M., *Performance Characteristics of a Centrifugal Pump Impeller with Running Tip Clearance Pumping Solid Liquid Mixtures*, Journal of Fluids Engineering, Vol.123, September 2001.

[19]You, D., Mittal, R., Wang, M., Moin, P., *Progress in Large Eddy Simulation of a Rotor Tip-Clearance Flow*, DOD HPCMP User Group Conference, Texas, 2002

[20]*Best Practice Guide for Turbomachinery,* Ansys CFX release 10.0, Ansys, Canada, 2005.

[21]Esch, T. and Menter, F.R., *Heat Transfer predictions based on two-equation models with advanced wall treatment*, Turbulence Heat and Mass Transfer, Antalya, Turkey, 2003

[22]Menter, F.R., *Turbulence Modeling for Turbomachinery*, QNET CFD Network Newsletter, Vol.2, No.3, December 2003.

[23]BS EN ISO 9906:2000, *Rotodynamic Pumps Hydraulic Performance Acceptance Tests, Grades 1 and 2*, October 2002.